Mine Water and the Environment (2019) 38:49–59
https://doi.org/10.1007/s10230-018-00573-2

TECHNICAL ARTICLE

Fine and Quantitative Evaluations of the Water Volumes in an Aquifer Above the Coal Seam Roof, Based on TEM

Kang Chen[1,2,3,4] · GuoQiang Xue[2,3,4] · WeiYing Chen[2,4] · NanNan Zhou[2,4] · Hai Li[2,4]

Received: 13 May 2017 / Accepted: 22 December 2018 / Published online: 3 January 2019

Abstract

A strategy to quantitatively evaluate the water content of aquifers was developed using transient electromagnetic (TEM) geo-electrical data and a database of generalized specific capacities obtained by pumping tests. Through regression analysis, a local (site-dependent) relationship was established between the generalized specific capacity and the aquifer's average resistivity. According to the relationship, the quasi-generalized specific capacity can be obtained using TEM data from across the entire survey area. The methodology was tested in a thick composite coal seam aquifer system with abundant water. By using the generalized specific capacities of 11 pumping wells and the average resistivities derived from TEM, a negative power function was established between the aquifer water volume and the area's resistivity. Using the quasi-generalized specific capacity provided a clearer understanding.

Keywords Transient electromagnetic method (TEM) · Water volumes · Quantitative estimate · Pumping test

Introduction

The average mining depth of the main state-owned coal mines in northern China exceeds 650 m (Peng 2008). These mines are not only threatened by the water in the shallow aquifers and goaf of the upper group coal seams, but are also seriously threatened by Ordovician, high-pressure karst water (Hu et al. 2010; Wu et al. 2013). With the increasing depth of coal mining in China, the difficulties involved in preventing and mitigating water-related disasters continues to be augmented.

There are many reasons for mine water accidents, but most are related to the abundant water in the goaf or aquifers (Bukowski 2011; Dong et al. 2007; Islam et al. 2005). With current geophysical technology, the spatial distributions of the water-enriched zone can be effectively detected (Jiang et al. 2007; Li et al. 2015; Xue et al. 2015), so we can control the water damage by drainage in advance. However, the faults and fissures generated during the mining processes frequently result in inrushes (Ma et al. 2000; Wu et al. 2013). It is therefore very important to precisely identify the water volumes of the aquifers located above and below the coal seams as a first step in preventing and controlling water damage.

Information related to the water abundance of aquifers is usually obtained from pumping test experiments (Bear 1988). Then, using data from the pumping tests, the specific capacities can calculated, which will quantitatively indicate the yield capacity of the aquifers (Hantush 1960, 1967). However, the hydrogeological data are often poorly distributed due to the high cost of pumping tests. Also, additional boreholes add potential underground watercourses, and increase the risk of water inrushes to the subsequent coal-mining processes (Wu et al. 2013). Most importantly, the regional hydrogeological parameters obtained by pumping

Electronic supplementary material The online version of this article (https://doi.org/10.1007/s10230-018-00573-2) contains supplementary material, which is available to authorized users.

✉ Kang Chen
chenkang_igg@126.com

1 State Key Laboratory of Simulation and Regulation of Water Cycle in River Basin, China Institute of Water Resources and Hydropower Research, Beijing 100038, China

2 Key Laboratory of Mineral Resources, Institute of Geology and Geophysics, Chinese Academy of Sciences, Beijing 100029, China

3 University of Chinese Academy of Sciences, Beijing 100049, China

4 Institutions of Earth Sciences, Chinese Academy of Sciences, Beijing 100029, China

tests are usually only average values. However, due to the heterogeneity of porous media, the mean values cannot reflect spatial variability (Lu 2015).The use of geophysical methods to obtain hydrogeological parameters will indirectly solve this problem, to some extent (Cassiani et al. 1997; Kelly 1977; Kelly et al. 1984; Niwas et al. 2011Ikard et al. 2016).

The transient electromagnetic (TEM) method is a geophysical exploration technique that is economical, efficient, and sensitive to low-resistivity bodies (Christensen et al. 1998). It has played an important role in hydrogeological prospecting (Robinson et al. 2008), as well as in preventing coal mine water damage (Liu et al. 2005; Hatherly 2013; Chang et al. 2017; Xue et al. 2018) over the last several decades. However, in the present study, based on the measured apparent resistivity values, the range and water volume of the aquifers (Goldman et al. 1994; Sumanovac et al. 2001), along with the spatial location of the water-containing goaf (Li et al. 2015; Xue et al. 2015), were only qualitatively obtained.

Scientists have been interested in the quantitative relationships between water volume and the electrical parameters (Danielsen et al. 2003; Yang et al. 2017). For example, Liu et al. (2010) established a physical experimental model to measure geoelectric parameters using a parallel electrical instrument. The results showed that apparent resistivity decreased with a negative power function when the water volume increased. By analyzing the relationship between the primary field current and water injection in the physical model, Liu et al. (2013) concluded that there was a positive correlation between the primary field current and the water yield of the detection area. However, most of the previous studies used very simple assumptions (a point flow source or sink in a uniform half-space), and the methods could not work well in actual in situ conditions. Therefore, additional methods and field measurements were needed to further develop these ideas.

In this study, we developed a quantitative method to evaluate the water content of aquifers using TEM data and quasi-generalized specific capacity. A formula of generalized specific capacity was deduced for a confined aquifer, and average resistivity was used to delineate the electrical characteristics of a confined aquifer. The new method was tested in a region of Inner Mongolia, where the hydrogeological and geophysical characteristics of the study area were analyzed in detail. The results of the new method were compared with those obtained using traditional methods. Finer quantitative information regarding the aquifer's water volume were obtained using the quasi-generalized specific capacities.

Methodology

Determination of the Yield Capacity of a Confined Aquifer

There are many types of aquifers with different characteristics. This study only deals with confined aquifers (Fig. 1). Groundwater flow can be described using the Theis formula (Domenico and Schwartz 1997), which does not theoretically create a steady flow. Therefore, if there is a stable period during a pumping test, it may have been caused by the water level slowly declining. This phenomenon can be expressed in the rate of the water level decline in the pumping well (Chen 1999) as follows:

$$\frac{ds_w}{dt} = \frac{Q}{4\pi T}\frac{1}{t}\exp\left(-\frac{\mu^{*2} r_w}{4Tt}\right) \approx \frac{Q}{4\pi T}\frac{1}{t} \tag{1}$$

where: s_w is drawdown (m); Q is discharge (m^3/day); T is transmissibility (m^2/day); t is time (day); μ^* is water storage coefficient; and r_w represents the radius of the pumping well (m). Since r_w is generally small, the conditions required for the above approximation are easily satisfied, as long as the pumping time is long enough. If a critical rate is used as a criterion for "stability" in the observational process, the critical time t_ξ (Chen 1999) is:

$$t_\xi = \frac{Q}{4\pi T \xi} \tag{2}$$

Specific capacity is obtained from a single well pumping test and can be used to evaluate the yield capacities of aquifers (Bear 1988; Samuel et al. 2003; Singh 2008). Specific capacity is defined as Q/Dh, where Q is the pumping rate and Dh is the drawdown. However, the direct observation of drawdown in pumping wells is a composite reflection, so

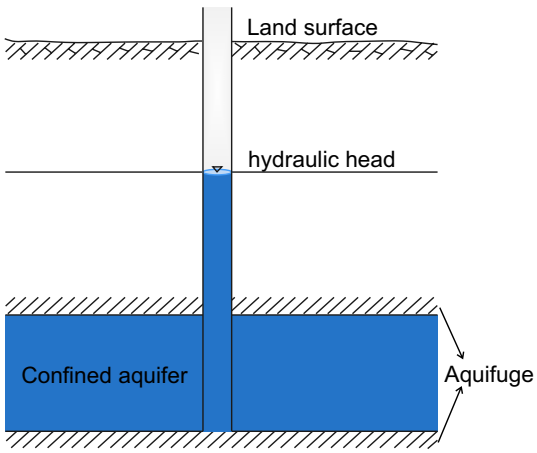

Fig. 1 Confined aquifer model

it is necessary to correct for the effect of well loss. Moreover, in order to facilitate comparison and analysis, a unified standard is needed to adopt to determine the water content of an aquifer, so it is necessary to convert diameter into a fixed value, especially when the difference of diameter between pumping wells is large (Zhou 2017). Therefore, scholars have extended this concept and proposed calculation methods for different hydrogeological conditions (Chen 1999; Priebe et al. 2018; Zhang et al. 2014), which is referred to here as the generalized specific capacity. In this study, a drawdown of 10 m in a borehole with a diameter of 91 mm was selected as a unified standard. The calculation formula for the generalized specific capacity of a confined aquifer (derivation shown in Chen 1999) is:

$$q_G = \frac{4\pi T}{\ln\left(2.25Tt_\xi/\left(\mu^* r_w^2\right)\right)} \approx \frac{4\pi T}{\ln\left(0.178Q_{91}/\left(\xi\mu^* r_w^2\right)\right)} \tag{3}$$

where $Q_{91} = Q_h\left(\frac{\lg R_h - \lg r_h}{\lg R_{91} - \lg r_{91}}\right)$, Q_{91}, R_{91}, and r_{91} are the water inflow, impact radius, and drilling radius of a well with a radius of 91 mm, respectively; and Q_h, R_h, and r_h are the water inflow, impact radius, and drilling radius of a well with the radius of r, respectively.

Electrical Characteristics of an Aquifer

According to the equivalent resistivity approximation theory, most rock can be considered to consist of uniformly connected cement and mineral grains with different shapes and pores (Waxman et al. 1968). The pores of rock in aquifers are filled with water. When the current flows through a rock mass, the difficulty with which ions flow through the rock pore system is known as the resistivity of the rock mass (Clavier et al. 1984). According to the classic Archie formula (Archie 1942):

$$\rho_t = \frac{1}{\phi^m S_w^n}\rho_w \tag{4}$$

where: ρ_t is the resistivity of the rock; φ is the porosity; S_w is the water saturation; ρ_w is the resistivity of the pore water; and m and n are the cementation and saturation indexes, respectively. In confined aquifers, the rock pores become filled with water; therefore $S_w = 1$. The values for m and n can be obtained from experimental data. In research studies, in order to examine hydrogeological conditions on a large scale, ρ_w is often assumed to be a constant (Kafri 2005). In this study, ρ_w was assumed to be an approximate invariant. Therefore, in accordance with Formula 4, it was assumed that: $\frac{\rho_w}{S_w^n} = A$, where A is a constant:

$$\rho_t = \frac{A}{\varphi^m} \tag{5}$$

An approximate relationship between ρ_t and φ^m was obtained. Then, using Formula (5), it was determined that the rock's porosity was inversely proportional to the bulk resistivity of the confined aquifer. That is to say, when porosity was small, the water content in the rock was low, resulting in high resistivity.

The electrical characteristics of an aquifer can be obtained quickly using the TEM method (Jiang et al. 2007; Robinson et al. 2008; Xue et al. 2015). In this study, a primary pulsed electromagnetic field of a certain waveform was transmitted through an ungrounded loop. During the intermittent period, an induced secondary eddy current field was observed with a coil or a grounded electrode. The analytical expression of the induced electromotive force in the central position (Nabighian 1988) was:

$$V(t) = -2\pi\mu_0 a^2 I \int_0^\infty L_p\left(\frac{1}{\lambda + u}\right)\lambda J_1(\lambda a) J_1(\lambda b) d\lambda \tag{6}$$

where $\frac{1}{\lambda+u} = \frac{\lambda}{\mu_0 \sigma s} - \frac{\sqrt{\left(s+\lambda^2/\mu_0\sigma\right)/\mu_0\sigma}}{s}$ and where the vacuum permeability, μ_0, is the earth's permeability; I represents the emission current; L_p is the transformation operator of Laplace; σ denotes the conductivity; λ is the integral variable; $J_1$is the first order Bessel function; and a, b are the radii of the transmitting and receiving loops, respectively. For the rectangular loop: $a = \sqrt{A/\pi}$.

According to Formula 6, the apparent resistivity formula (Li 2002) is:

$$\rho(t_i) = \frac{\mu_0}{4\pi t_i}\left[\frac{2\mu_0 Mq}{5t_i V(t_i)}\right]^{\frac{2}{3}} \tag{7}$$

where the subscript, i, of time, t, is the number of observational time channels; Mis the magnetic moment of the transmitter loop; and q is the effective area of the receiving coil. The corresponding apparent depth,h, can be calculated using the following equation (Spies 1989):

$$h = \sqrt{\frac{\rho(t_i) \times t_i}{2\mu_0}} \tag{8}$$

A confined aquifer is a layered body that has a certain thickness (Fig. 1). The electrical characteristics of the aquifer cannot be accurately defined by the apparent resistivity of a certain depth. Hence, we needed to determine the electromagnetic response, as well as its time, which corresponded to the depth and thickness of the aquifer. Therefore, the corresponding resistivity, ρ_i, and depth, h_i, were calculated using Formulas 7 and 8. The average resistivity $\bar{\rho}$ of the aquifer could then be determined by the following relationship:

$$\bar{\rho} = \frac{\sum_{i=1}^n \rho_i h_i}{\sum_{i=1}^n h_i} \tag{9}$$

where $i = 1, 2, \ldots\ldots, n$; and n is the number of points to be calculated based on the depth and thickness of the confined aquifer.

Estimating the Water Volumes of an Aquifer

Based on the previous analysis, a pumping test was conducted to study the aquifer. The measured data after processing were substituted into Formula 3, and the generalized specific capacities q_G were obtained, by which the water content of the aquifer was determined at a drilling location. A TEM survey was also conducted at the drilling position. Then, based on the characteristics of the aquifer, the measured data after processing were substituted into Formula 9, and the average resistivity $\bar{\rho}$ was obtained, which better reflected the electrical characteristics of the aquifer.

Furthermore, in order to obtain a fine estimate of the aquifer's water content, a regression analysis of the average resistivity $\bar{\rho}$ and generalized specific capacity, $q_G w$, was performed. The general relational expression for the regression analysis was described as follows (Kumar et al. 2008):

$$y = \varphi\left(x_1, x_2, ..., x_m, \beta_1, \beta_2, ..., \beta_i\right) + \varepsilon \tag{10}$$

For the set of the field data $\left(\bar{\rho}_i, q_{Gi}\right), i = 1, 2, ..., n$, expression 11 was rewritten as:

$$q_{Gi} = f\left(\bar{\rho}_i, \theta\right) + \varepsilon_i \quad i = 1, 2, ..., n \tag{11}$$

where θ is an unknown parameter vector and ε_i is a random error term that satisfies the independent and identical distribution assumption. Therefore, when the function f was assumed to be continuously differentiable to θ, a differential method was used to establish the normal equations, and θ was allowed to reach a minimum:

$$Q(\theta) = \sum_{i=1}^{n} \left(q_{Gi} - f\left(\bar{\rho}_i, \theta\right)\right)^2 \tag{12}$$

Then, function Q was used to derive the parameter θ_j and make it equal to 0, and the $p + 1$ equation was obtained:

$$\left.\frac{\partial Q}{\partial \theta_j}\right|_{\theta_j = \hat{\theta}_j} = -2 \sum_{i=1}^{n} \left(q_{Gi} - f\left(\bar{\rho}_i, \hat{\theta}\right)\right) \left.\frac{\partial f}{\partial \theta_j}\right|_{\theta_j = \hat{\theta}_j} = 0 \quad j = 0, 1, 2, ..., p \tag{13}$$

The least squares estimation of $\hat{\theta}$ was the solution of Formula 12 (Keith 2014). Finally, the regression equation of $\bar{\rho}$ and q_G was obtained. The electromagnetic responses measured by TEM over the entire area were processed using the method described above in order to obtain the average resistivity, $\bar{\rho}$. Then, the average resistivity $\bar{\rho}$ were substituted into regression Formula 13 to obtain the quasi-generalized specific capacities $\widehat{q}_G$ at each survey point. Finally, this study quantitatively and closely examined the water volumes of the aquifer over the entire area using the quasi-generalized specific capacities $\widehat{q}_G$.

Field Experiment

The methodology described in the previous section was applied to a real scenario (Fig. 2). The survey area was located in the Hailar District of Hulunbeier City, China (Fig. 3). The experiment consisted of a classical pumping test. Also, the transient electromagnetic responses at the ground surface were measured.

Hydrogeological Characteristics of the Region

The measurement was carried out at approximately 15 km^2. The coal-bearing strata in the tendency direction were basically flat, and the inclination was less than 5°. According to the drilling data, the main mining coal seam 15-1 was located in the upper part of the Yimin Formation, which was stable and continuous. The average thickness of the main mining seam was 5.46 m. The upper part of the main coal seam had a thick confined aquifer containing sandstone and conglomerate. Also, the aquifuge which separated the aquifer from the coal was thin, and was discontinuous in the entire area. The hydrogeological characteristics of this area were analyzed as follows:

1. The Quaternary aquifer was mainly composed of fine and medium-coarse sand, and gravel, which contained less water (Fig. 4).
2. The Quaternary aquifuge mainly consisted of discontinuous clay, silty clay, calcareous clay, and other components. The average thickness was 10.75 m. The middle part of the Quaternary aquifuge was thick (Fig. 4).
3. The upper aquifer was the primarily aquifer, which was distributed from the bottom of the Quaternary to the 15-1 coal roof (Fig. 4). The aquifer in the central north section was thick, and was observed to be thin in the

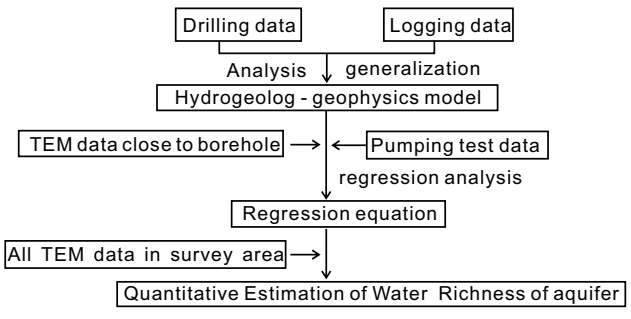

Fig. 2 Flow chart of quantitative estimation of water volumes of aquifers

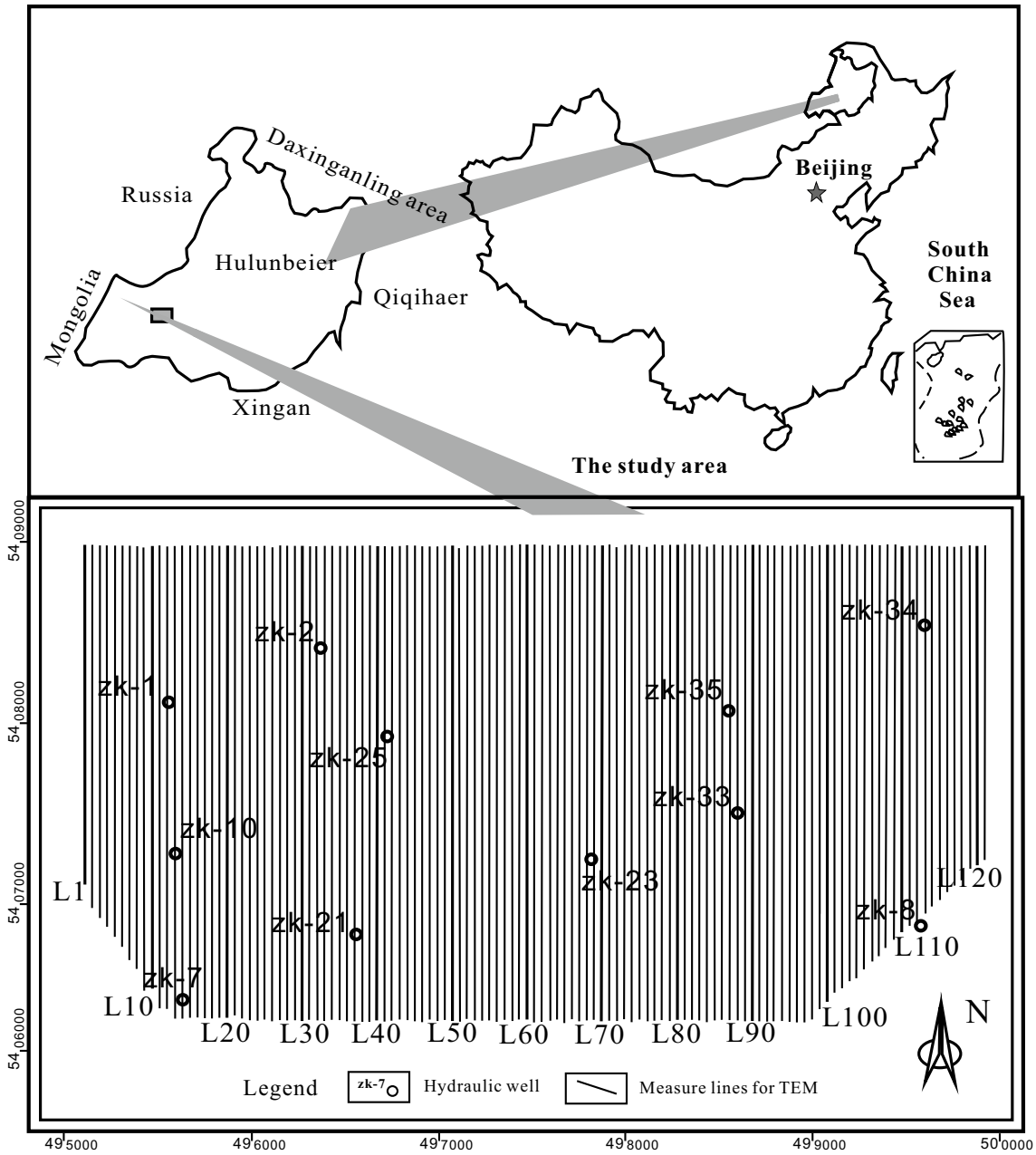

Fig. 3 Layout of project

southeast and southwest sections (Supplemental Fig. 1). The groundwater flow direction was generally from east to west. The west and northwest sections were the main discharge zones (Supplemental Fig. 2). By observing the core, it was found that the northwest aquifer was thick, and the lithology was dominated by mainly sandstone and conglomerate. Moreover, the cement was found to be loose, with large porosity, and the permeability was determined to be good. However, the aquifer in the southeastern part was thin, and the lithology was dominated by sandstone, with fewer conglomerates observed. The porosity and permeability were determined to be moderate (Supplemental Fig. 3).

4. The coal seam roof aquifuge did not exist throughout the entire study area. It was found to be widespread in the southeast and southern sections, and thinner in the northwest section (Fig. 4).

Therefore, by the above analysis, it was determined that the upper aquifer was thick, and had abundant water. The upper aquifer received recharge from the Quaternary aquifer. Furthermore, the coal seam roof aquifuge was not

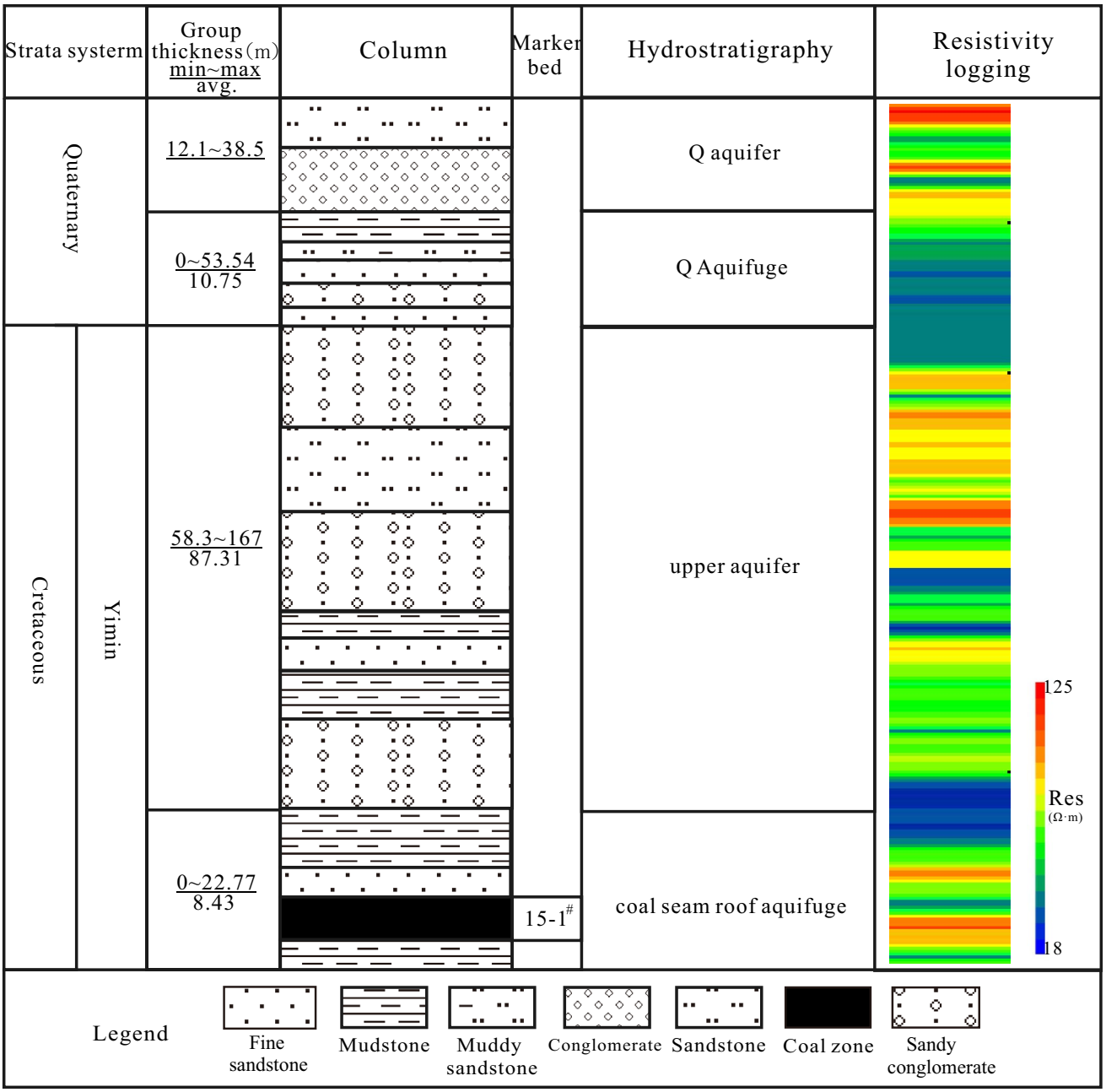

Fig. 4 Delineation of hydrogeological–geophysical model

continuous. Therefore, the 15-1 coal seam was seriously affected by the water volume of the upper aquifer. Also, since the study area was large, the TEM method was determined to be a good choice for accurately studying the characteristics of the aquifer water content in the study region.

Geophysical Characteristics of the Region

As can be seen in Table 1, the resistivity of the rock was obviously variable in the study area, and the coal seam had a high resistance value. Also, the formation water greatly influenced the overall resistivity response of the rock. Therefore, TEM was used to analyze and evaluate the water

content of the formation. Then, by using a comprehensive analysis of the hydrogeological conditions and logging data, a summarized hydrogeological and geophysical model of the region was constructed (Fig. 4).

Description of the Experiment

Due to the large scope of the study area, the electromagnetic response and specific capacity were measured at 11 evenly drilled boreholes distributed throughout the area (Fig. 3), rather than at just one location. Then, pumping tests were conducted in order to obtain specific capacity data in each borehole to accurately and quantitatively estimate the aquifer's water content.

This study used a Phoenix V8 multi-function electromagnetism system (Canada), with a total of 121 lines arranged along a north–south direction. The exploration grid was 40 m (line spacing) × 20 m (dot pitch). The device and the parameters of this test are shown in Table 2. The vertical inductive voltage was measured using a magnetic probe, which effectively covered a receiving area of 1000 m^2.

Results and Discussion

Analysis of the Pumping Test Results

According to China's Coal Field Hydrogeological Norms, an area in which the specific capacity is greater than 1 L/(s·m) has strong water abundance and is prone to flooding accidents. Therefore, it is necessary to carry out drainage work in advance. We obtained the generalized specific capacities (Table 3) of the study area by analyzing and processing the hydrological borehole pumping data (Chen 1999; Jiao 2006). Then, a contour map of the generalized specific capacities of the entire study area was completed by interpolation (Fig. 5).

The water abundance of the upper aquifer in the study area was unevenly distributed (Fig. 5). The water volume was strongest in the middle section, and the generalized specific capacity was ≈ 1.6 L/(s·m). Also, the aquifer's water content was observed to gradually decrease in the surrounding area and was weakest in the eastern section, where the specific capacity was below 1 L/(s·m), and the risk of water damage was relatively low. However, the specific capacities were more than 1 L/(s·m) in the other three directions, which also had high water content.

Given the large scope of the study area, there was relatively little pumping test data, and the regional hydrogeological parameters were usually only averaged values (estimated by interpolation). However, due to the complex hydrogeological conditions of the study area, the mean values could not reflect local variability.

Table 1 statistics of apparent resistivity of rocks in the area

Lithology	Average apparent resistivity (Ω m)
Clay	13
Mudstone	22
Siltstone	35
Fine sandstone	25
Coal	65
Coarse sandstone	74
Conglomerate	78

Table 2 Measurements datasheets of TEM

Category	Selected parameters
Measuring device	Fixed loop
Transmitter wireframe (m)	360 × 360
Transmission frequency (Hz)	5
Supply current (A)	10 ± 0.5
Observation time (min)	2 ~ 3
Receiving window (ms)	0.1–47.5

Analysis of the TEM Results

When using TEM to study the water content of an aquifer, a resistivity contour map is usually used for qualitative judgments (Jiang et al. 2007; Xue et al. 2015). Therefore, using the measured data, we compared the results using the new, proposed method with the more traditional method. Also, a depth of − 150 m was selected, based on the hydrogeological features of this area (Supplemental Fig. 3), to illustrate the resistivity results. At that depth (Fig. 6), it can be seen that the resistivity varies greatly, and a clear partition is evident. The resistivity in the central part of the study area was observed to be high. Therefore, by selecting a resistivity of less than 25 Ω *m*as a division standard, there were

Table 3 Pumping test results table for the upper aquifer

Number	Generalized specific capacity q_G [l/(s m)]	Number	Generalized specific capacity q_G [l/(s m)]
zk-1	1.42	zk-23	1.55
zk-2	1.45	zk-25	1.65
zk-7	1.35	zk-33	1.61
zk-8	0.73	zk-34	0.94
zk-10	1.62	zk-35	1.42
zk-21	1.61		

The specific capacity has been converted into a unified standard data of 91 mm diameter

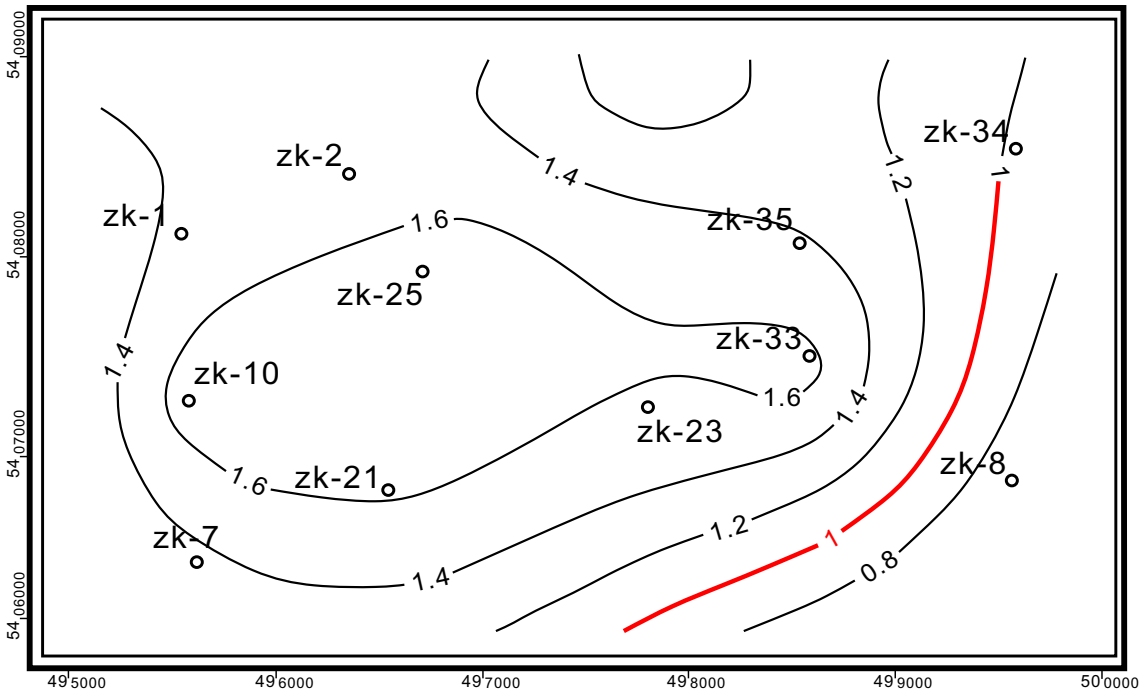

Fig. 5 Contour map of the generalized specific capacity (According to the water abundance area division standard, the area that the generalized specific capacity is greater than 1 $l/(s\ m)$ is strong water abundance area)

three obvious low resistance zones observed in the eastern, middle-northern, and southwest sections. Also, these three areas were determined to be strong water content areas, when judged only by the resistivity contour map.

When the results shown in Figs. 5 and 6 are compared, one can see that the water abundance obtained using the traditional method did not agree well with the pumping test results. This was because there were many factors that affects resistivity, including lithology, pore structure, and water content. Furthermore, the upper aquifer in the study area was a composite aquifer, and the distribution of the rock was not uniform. Therefore, the traditional method may have been biased by the resistivity contours of the depth used to analyze the aquifer's water volumes.

Quantitative Estimation of the Water Volumes of the Aquifer for the Entire Study Area

Using the new method proposed above, the data from the 11 boreholes were analyzed and processed, and 11 generalized specific capacities were obtained (Table 3). Then, by using the electromotive force data measured near the 11 boreholes, along with Formulas 7 and 8, the apparent resistivity values at the different depths of those positions were obtained. Through analysis of the depth and thickness of the aquifer at each location (using the drilling data), and substituting the apparent resistivity values corresponding to the depths into Eq. 9, the average resistivity of each location was obtained. Furthermore, by using regression analysis to analyze the 11 data sets, a suitable correlation equation was acquired (Fig. 7). It was found that between the generalized specific capacity and the average resistivity, $y = 1064.1x^{-1.92}$. Also, the correlation coefficient was determined to be $R^2 = 0.919$. In order to quickly and accurately obtain the aquifer water abundance areas within the entire region, the average resistivity of all the TEM measuring points that corresponded to the upper aquifer in the region were calculated. Then, the average resistivity values were substituted into the regression equation $y = 1064.1x^{-1.92}$ to obtain the quasi-generalized specific capacity $\widehat{q}_{\mathrm{G}}$.

To better illustrate the feasibility and superiority of the new method, a contour map for the quasi-generalized specific capacity $\widehat{q}_{\mathrm{G}}$ was constructed, and then combined with the contour map of the measured generalized specific capacity q_G (Fig. 5) for comparison (Fig. 8). The two variables were generally found to be consistent in reflecting the aquifer's water content. For example, in the central, western, and northeastern areas, the water volume of the aquifer was large, which had a major impact on the mining of the coal seams. In the eastern and southeastern parts of the survey area, the water-bearing capacity of the aquifer was weaker. Therefore, due to the large data density, the contour map of the quasi-generalized specific capacity $\widehat{q}_{\mathrm{G}}$ better reflected the actual situation in the study area.

In Fig. 8, the closed red line marks the region in which the quasi-generalized specific capacity $\widehat{q}_{\mathrm{G}}$ was less than

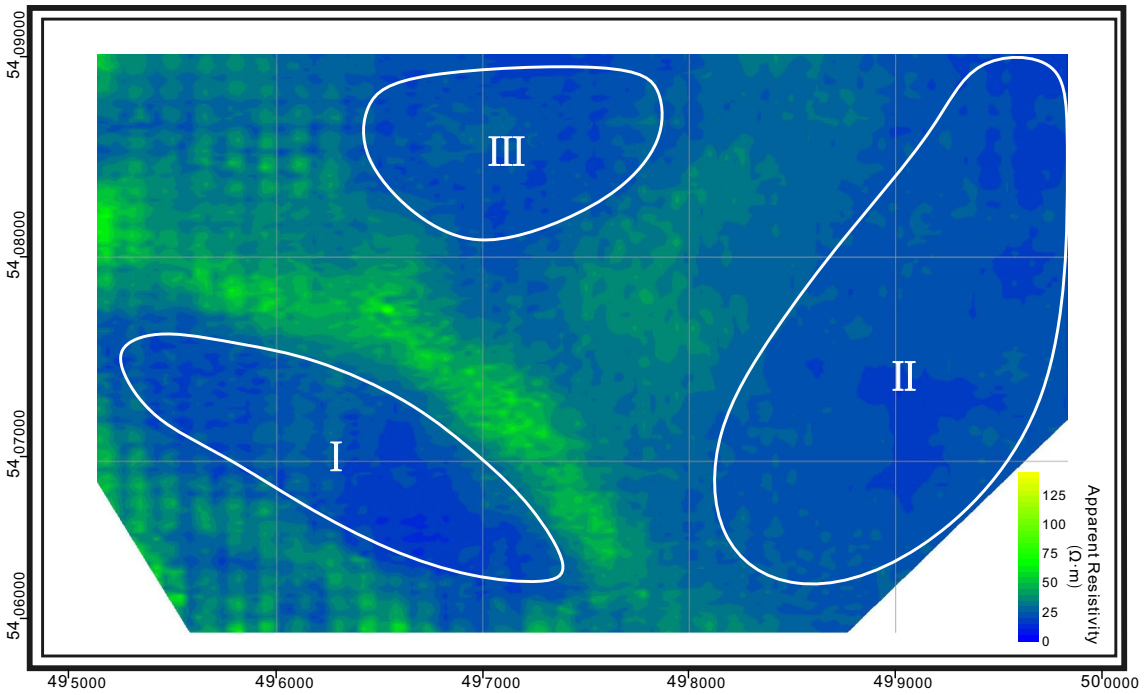

Fig. 6 Apparent resistivity slice map for − 150m

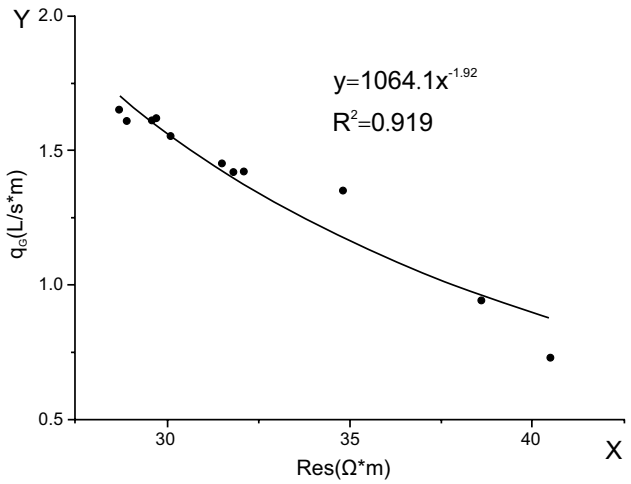

Fig. 7 Correlation and regression analysis of average apparent resistivity and generalized specific capacity

1 L/(s·m), which indicated that the area was relatively safe. In the middle of contour map, where q_G was higher than 1.6 L/(s·m), there were several areas with $\widehat{q}_G$ less than 1 L/(s·m). Meanwhile, there were also relatively safe areas in the northwestern and eastern sections of the survey area. This showed that a more detailed water volume distribution could be obtained, along with a better understanding of the actual situation, when the quasi-generalized specific capacity $\widehat{q}_G$ was utilized. In this way, prior to coal mining, the exploration and mine dewatering could be conducted in a more efficient and economical manner.

Conclusions

A quantitative method to evaluate aquifer water volumes based on TEM was developed in this study. In view of the specific characteristics of confined aquifers, a formula to solve the generalized specific capacity in an entire area was proposed. Then, using TEM data, the rarely measured generalized specific capacities were extended into a quasi-generalized specific capacity, by which the water volume of a confined aquifer could be obtained more accurately.

The proposed procedure was then applied to a coal mine in Inner Mongolia, where the hydrogeology is relatively complex. For this specific example, a simple relationship between the average apparent resistivity and the generalized specific capacity was established. However, it was important to adjust the predictive formula based on the field data for the specific site, since the valid application region of the equation was limited by the site's hydrogeological characteristics. The results using the new and traditional methods were compared, and better quantitative information regarding the water volumes of the confined aquifer were obtained using the quasi-generalized specific capacities. These will potentially be used to provide a reliable reference to guide underground water exploration and

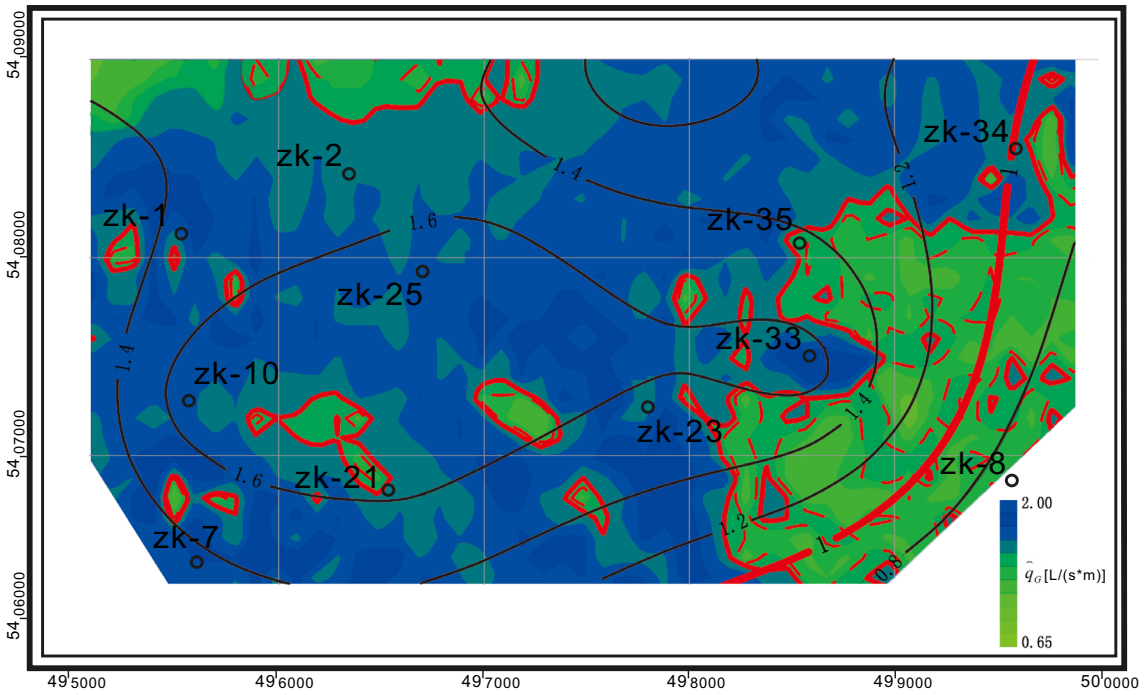

Fig. 8 Comparison of contour map of $\widehat{q}_G$ and q_G (the area filled with colors represents the quasi generalized specific capacity $\widehat{q}_G$, with the value increasing from green to blue. And the closed red line is used to mark areas of the aquifer with $\widehat{q}_G$ of less than 1 $l/(s\,m)$. The line marked with the value is the contour of measured generalized specific capacity q_G)

geophysical activities during mining. At the same time, our test showed that the traditional method, which used a resistivity contour map at a certain depth to analyze the aquifer's water volumes may have possibly resulted in erroneous judgments. Moreover, the results also provided a viable method for quantitatively judging the water content of aquifers using electromagnetics.

In the future, we hope to further improve the model relative to generalized specific capacity and apparent resistivity to allow dynamic monitoring of groundwater in coal mines using a combination of data obtained from long-term observations of hydrogeological boreholes and TEM.

Acknowledgements This research was supported by the National Key Research and Development Program of China (2017YFC0601204), the National Natural Science Foundation of China (41474095), and the Open Foundation of Key Laboratory of Mineral Resources, Chinese Academy of Sciences (KLMR2015-09).

References

Archie GE (1942) The electrical resistivity log as an aid in determining some reservoir characteristics. Trans AIME 146(01):54–62

Bear J (1988) Dynamic of fluids in porous media. McGraw-Hill, New York

Bukowski P (2011) Water hazard assessment in active shafts in Upper Silesian Coal Basin Mines. Mine Water Environ 30(4):302–311

Cassiani G, Medina MA (1997) Incorporating auxiliary geophysical data into groundwater flow parameter estimation. Ground Water 35(1):79–91

Chang J, Yu J, Su B (2017) Numerical simulation and application of mine TEM detection in a hidden water-bearing coal mine collapse column. J Environ Eng Geophys 22(4):223–234

Chen CX, Lin M (1999) Groundwater dynamics. China University of Geosciences Press, Wuhan **(in Chinese)**

Christensen NB, Sørensen KI (1998) Surface and borehole electric and electromagnetic methods for hydrogeological investigations. Eur J Environ Eng Geophys 3:75–90

Clavier C, Coates G, Dumanoir J (1984) Theoretical and experimental bases for the dual-water model for interpretation of shaly sands. Soc Petrol Eng J 24(02):153–168

Danielsen JE, Auken E, Jørgensen F, Søndergaard V, Sørensen KI (2003) The application of the transient electromagnetic method in hydrogeophysical surveys. J Appl Geophys 53(4):181–198

Domenico PA, Schwartz FW (1997) Physical and chemical hydrogeology. Wiley, New York City

Dong S, Hu W (2007) Basic characteristics and main controlling factors of coal mine water hazard in China. Coal Geol Explor 35(5):34–38 **(in Chinese)**

Goldman M, Rabinovich B, Rabinovich M, Gilad D, Gev I, Schirov M (1994) Application of the integrated NMR-TDEM method in groundwater exploration in Israel. J Appl Geophys 31(1):27–52

Hantush MS (1960) Modification of the theory of leaky aquifers. J Geophys Res 65(11):3713–3725
Hantush MS (1967) Flow of groundwater in relatively thick leaky aquifers. Water Resour Res 3(2):583–590
Hatherly P (2013) Overview on the application of geophysics in coal mining. Int J Coal Geol 114:74–84
Hu WY, Tian G (2010) Mine water disaster type and prevention and control countermeasures in China. Coal Sci Technol 1:45–47 **(in Chinese)**
Ikard SJ, Kress W (2016) Electric-hydraulic correlations in layered aquifers: a case study of the surficial aquifer of Emirate Abu Dhabi, United Arab Emirates. J Environ Eng Geophys 21(4):187–200
Islam MR, Islam MS (2005) Water inrush hazard in Barapukuria coal mine, Dinajpur District, Bangladesh. Bangladesh J Geol 24(1):1–17
Jiang ZH, Yue JH, Liu ZX (2007) Application of mine transient electromagnetic method in forecasting goaf water. Chin J Eng Geophys 4(4):291–294 **(in Chinese)**
Jiao Y (2006) Improvement of routine method to define influential radius in leaky confined aquifer. Rock Soil Mech 29(10):2779–2782 **(in Chinese)**
Kafri U, Goldman M (2005) The use of the time domain electromagnetic method to delineate saline groundwater in granular and carbonate aquifers and to evaluate their porosity. J Appl Geophys 57(3):167–178
Keith TZ (2014) Multiple regression and beyond: an introduction to multiple regression and structural equation modeling. Routledge, London
Kelly WE (1977) Geoelectric sounding for estimating aquifer hydraulic conductivity. Groundwater 15(6):420–425
Kelly WE, Reiter PF (1984) Influence of anisotropy on relations between electrical and hydraulic properties of aquifers. J Hydrol 74(3–4):311–321
Kumar KV, Porkodi K, Rocha F (2008) Isotherms and thermodynamics by linear and non-linear regression analysis for the sorption of methylene blue onto activated carbon: comparison of various error functions. J Hazard Mater 151(2):794–804
Li X (2002) The theory and application of transient electromagnetic sounding. Shaanxi Science Technology Press, Xi'an **(in Chinese)**
Li H, Xue GQ, Zhou NN, Chen WY (2015) Appraisal of an array TEM method in detecting a mined-out area beneath a conductive layer. Pure Appl Geophys 172(10):2917–2929
Liu SC, Liu ZX, Jang ZH (2005) Application of TEM in hydrogeological prospecting of mining district. J China Univ Min Technol 34(4):414 **(in Chinese)**
Liu S, Yang S, Cao Y, Liu J (2010) Analysis about response of geoelectric field parameters to water inrush volume from coal seam roof. J Min Safety Eng 27(3):341–345 **(in Chinese)**
Liu J, Liu S, Cao Y, Yang S (2013) Quantitative study of geoelectric parameter response to groundwater seepage. Chin J Rock Mech Eng 32(5):986–993 **(in Chinese)**
Lu DB (2015) Subsurface visualization and monitor technique based on electrical resistivity tomography for complicated topography. Nanjing University, Nanjing **(in Chinese)**
Ma Y, Wu Q, Zhang Z (2000) Research on prediction of water conducted fissure height in roof of coal mining seam. Coal Sci Technol 36(05):59–62 **(in Chinese)**
Nabighian MN (1988) Electromagnetic methods in applied geophysics: theory, vol 1. Society of Exploration Geophysicists, Tulsa
Niwas S, Tezkan B, Israil M (2011) Aquifer hydraulic conductivity estimation from surface geoelectrical measurements for Krauthausen test site, Germany. Hydrogeol J 19(2):307–315
Peng SP (2008) Present study and development trend of the deepen coal resource distribution and mining geologic evaluation. Coal 17(2):1–11 **(in Chinese)**
Priebe EH, Neville CJ, Rudolph DL (2018) Enhancing the spatial coverage of a regional high-quality hydraulic conductivity dataset with estimates made from domestic water-well specific-capacity tests. Hydrogeol J 26(3):395–405
Robinson DA, Binley A, Crook N, Day LFD, Ferré TPA, Grauch VJS, Nyquist J (2008) Advancing process-based watershed hydrological research using near-surface geophysics: a vision for, and review of, electrical and magnetic geophysical methods. Hydrol Proc 22(18):3604–3635
Samuel MP, Jha MK (2003) Estimation of aquifer parameters from pumping test data by genetic algorithm optimization technique. J Irrig Drain Eng 129(5):348–359
Singh SK (2008) Estimating aquifer parameters from early drawdowns in large-diameter wells. J Irrig Drain Eng 134(3):409–413
Spies BR (1989) Depth of investigation in electromagnetic sounding method. Geophysics 54:872–888
Šumanovac F, Weisser M (2001) Evaluation of resistivity and seismic methods for hydrogeological mapping in karst terrains. J Appl Geophys 47(1):13–28
Waxman MH, Smits LJM (1968) Electrical conductivities in oil-bearing shaly sands. Soc Petrol Eng J 8(02):107–122
Wu J, Cui FP, Zhao SQ, Liu SJ, Ceng YF, Gu YW (2013) Type classification and main characteristics of mine water disasters. J Chin Coal Soc 38(4):561–565 **(in Chinese)**
Xue GQ, Li X, Gelius LJ, Qi ZP, Zhou NN, Chen WY (2015) A new apparent resistivity formula for in-loop fast sounding TEM theory and application. J Environ Eng Geophys 20(2):107–118
Xue G, Chen W, Ma Z, Hou D (2018) Identifying deep coal-bed water-filled zones in China through the use of large loop TEM. J Environ Eng Geophys 23(1):135–142
Yang C, Liu S, Wu R (2017) Quantitative prediction of water volumes within a coal mine underlying limestone strata using geophysical methods. Mine Water Environ 36(1):51–58
Zhang J, Wang XS (2014) Multiple solutions of specific capacity for pumping wells and their application. Geotech Invest Surv 3:33–37
Zhou X (2017) The specific well capacity is not the same as the transmissivity of the aquifer tapped by the well-for discussion with Mr. Lan Taiquan. Hydrogeol Eng Geol 44(2):184–188